A CPW-fed Triple-band Antenna for WLAN and WiMAX Applications

Xiaolin YANG, Fangling KONG, Xuelin LIU, Chunyan SONG

Dept. of Physics and Electronics, University of Electronic Science and Technology of China,
No.4, Section 2, North Jianshe Road, 610054 ChengDu, SiChuan

yxlin@uestc.edu.cn, 770311315@qq.com, 595476221@qq.com, 331020368@qq.com

Abstract. *In this letter, a compact printed antenna fed by coplanar waveguide for triple-band is presented. The proposed antenna consists of two rectangular metallic loops in front and a slit square ring on the backside. Tri-band has been achieved, which can be easily tuned by adjusting the sizes of the rectangles. An analysis of equal lumped circuit mechanism as well the triple band operation is provided. Key parameters to tune the resonant frequencies have been identified. The overall dimension of the proposed antenna is 30 × 26 mm^2. Simulated results show that the presented antenna can cover three separated impedance bandwidths of ~13% at 300 MHz (2.2–2.5 GHz), ~14% at 500 MHz (3.3–3.8 GHz), and ~15% at 800 MHz (5.1–5.9 GHz), which are well applied for both 2.4/5.2/5.8-GHz WLAN bands and 3.5/5.5-GHz WiMAX bands.*

Keywords

Triple-band, coplanar waveguide, equivalent circuit.

1. Introduction

With the development of wireless communication technology, demand for designing an antenna with multi-band operation performance has increased rapidly since such an antenna is vital for integrating more than one communication standards in a single compact system which can effectively promote the portability of a modern personal communication system. Furthermore, mitigate the size of antenna is particularly important for the antenna designer. Owing to its properties, such as low cost, light weight, simple fabrication and compact size, monopole planar antennas are considered to be the best choice for multiband applications.

Many kinds of multi-band antennas have been reported in papers. A tri-band antenna with complicated ground and multiple metallic strips is reported in [1]. Some multi-band antennas are realized by cutting slots such as H-shaped [2], U-shaped [3]–[5], and many other shapes [6]–[8] in the radiating patch or ground, which can introduce different electrical paths. Strips with different length are also used in some letters, and different resonant frequency can be obtained by adjusting the length of them [9]–[11]. However, these methods have drawbacks, namely increasing the physical size of antenna and creating undesired radiation from parasitic elements.

Recently, several multiple bands antennas have been developed. A quadruple-band elliptical antenna for WiMAX applications is reported in [13]. It was found good performance at four bands. However, it may be difficult to adjust and analysis each band dependently for they are introduced by one resonant element (i.e. the sector slot). Moreover, a triple-band antenna is studied in [14]. The reflection coefficient at three bands reaches -25 dB. But for the frequency outside the multi-bands the band-notched performance is bad (S11 < -5 dB) and the size is a little big for its stereo structure.

In this paper, a monopole antenna with coplanar waveguide (CPW) feed line is presented, which exhibits multi-frequency functionality by using two square electrical paths of different lengths and a parasitic split rectangular loop in backside. These three specific shaped structures and their coupling property introduce two distinct resonant modes, and the slit square loop on backside not only plays a role of band-notched function, but also improves the impedance matching at 5.5 GHz. The measured results show good agreement with the simulated ones, which demonstrates that the antenna shows a good multiband characteristic to satisfy the requirement of WLAN in the 2.4/5.2/5.8-GHz bands and WiMAX in the 3.5/5.5-GHz bands. Details of the designed antenna are described in the paper, and both simulated and measured results are presented. Good multi-bands and notched-bands characteristics are obtained when compared to the design in [14]. Furthermore, the size is reduced significantly.

2. Antenna Design and Implementation

Fig. 1(a) shows the geometry of the presented triple-band antenna. The photograph of the fabricated antenna is displayed in Fig. 1(b). A 50 Ω CPW transmission line (with width of 3.8 mm and a gap of 0.2 mm between the feed line and the ground plane) and two square loops are printed on top of the substrate whose dielectric constant is 2.65 and the thickness is 0.8 mm, and a slit rectangular ring is

printed on the back side of the substrate. The overall size of the proposed antenna reaches only 30 × 26 mm^2.

Their reflection coefficient is shown in Fig. 2(b) respectively. Because the length of the first square loop is $L_1 + W_3/2$ which is about one-fourth wavelength at 3 GHz but half wavelength at 5.8 GHz. Similarly to the half wavelength dipole antenna, dual-band is introduced. Compared to the Step1, a notched band at 2.7 GHz and one-band at 3.55 GHz are introduced after adding the rectangular ring to the Step1.The length of the slot between the two rectangular rings is $L_1 - 2W_1 + W_3/2$ which is about quarter wavelength at 2.7 GHz. It can be equaled to an open-ended quarter wavelength transmission line which operates as a series resonance circuit. To the frequency at 3.55 GHz, the length

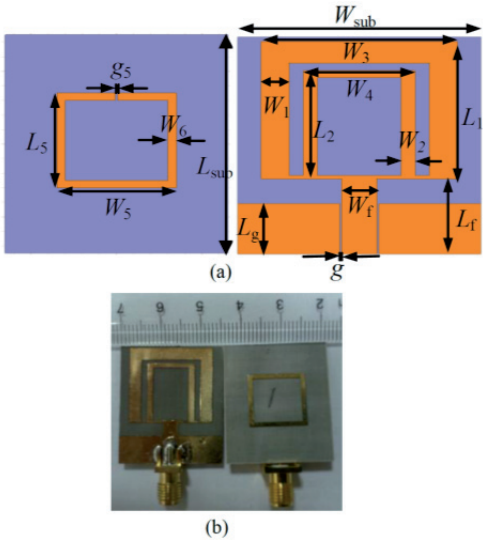

Fig. 1. (a) Geometry of the proposed antenna.
(b) Photograph of tri-band antenna.

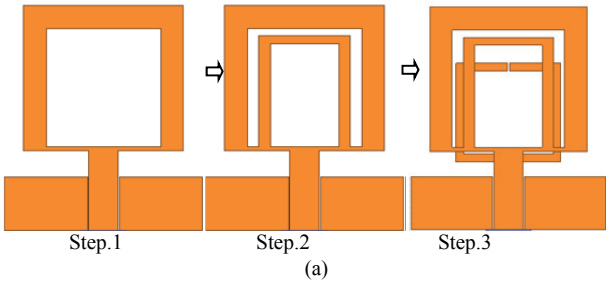

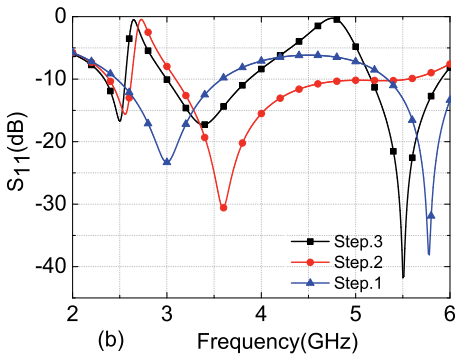

Fig. 2. (a) Process of designing ultimate antenna.
(b) Simulated reflection coefficient of Step 1 to 3.

of the inner rectangular loop is larger than quarter wavelength but a little less than half wavelength. So it can be treated as a parallel circuit with finite resistance. The reflection coefficient becomes larger than -10 dB at 5.6 GHz, which is about -40 dB as for Step1. Due to the similar reason, the length of the slot equals to half wavelength at 5.6 GHz, a parallel resonance circuit with finite resistance is introduced.

To further widen the bandwidth at 3.6 GHz, a series resonance circuit is recommended. The corresponding conceptual equivalent circuit model is shown in Fig. 3. Z_{A1} represents the complex input impedance of Step1. R_{eqi}, L_{eqi} and C_{eqi} (i = 1, 2, 3, 4) are the resistor, inductor and capacitor values of the series and parallel resonant circuits respectively.

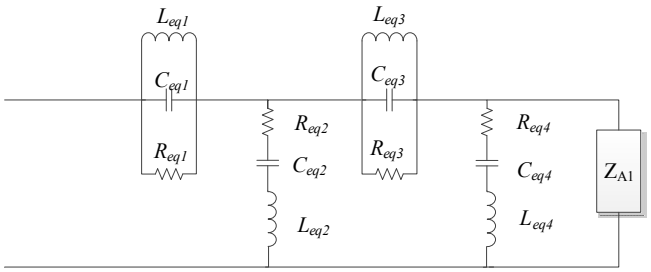

Fig. 3. Equivalent circuit model of Step1 to Step 2.
R_{eq1} = 43.3 Ohm, C_{eq1} = 5.5 pF, L_{eq1} = 0.38 nH,
R_{eq2} = 0.0001 Ohm, C_{eq2} = 0.108 pF, L_{eq2} = 29.2 nH,
R_{eq3} = 48 Ohm, C_{eq3} = 3.71 pF, L_{eq3} = 0.21 nH,
R_{eq4} = 104.96 Ohm, C_{eq4} = 0.38 pF, L_{eq4} = 4.96 nH.

All the values of the circuit are calculated by the following formulas [12]:

The value of the series resonant circuit is given by

$$BW = \frac{1}{Q} = \frac{R}{\omega_0 L} = 2\frac{\Delta\omega}{\omega_0}, \tag{1}$$

$$\omega_0 = \frac{1}{\sqrt{LC}}. \tag{2}$$

Here BW equals to the -3dB bandwidth.

As for the parallel resonant circuit, the resonant frequency and bandwidth can be predicted by using the formulas given in:

$$BW = \frac{1}{Q} = \frac{1}{\omega_0 RC} = 2\frac{\Delta\omega}{\omega_0}, \tag{3}$$

$$\omega_0 = \frac{1}{\sqrt{LC}}. \tag{4}$$

After the initial values of R_{eqi}, L_{eqi} and C_{eqi} (i = 1, 2, 3, 4) are calculated by using the equations (1)-(4), the equivalent circuit is built, tuned and optimized in ADS 2009 software package. The calculated and simulated input impedance and reflection coefficient of the equivalent circuit is compared in Fig. 4(a)–(c), in which a reasonable agreement can be observed.

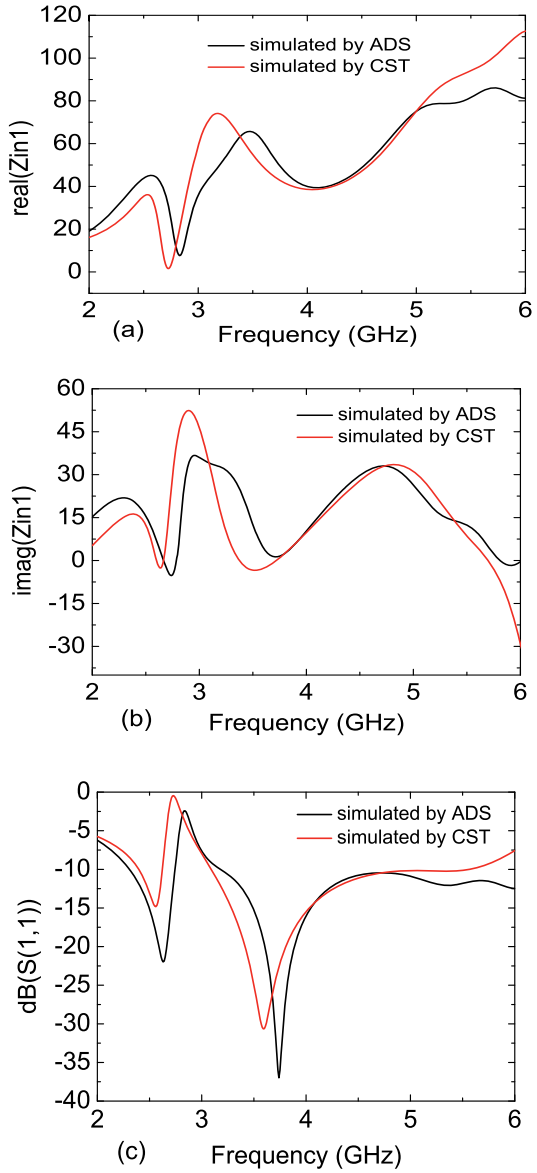

Fig. 4. Impedance and reflection coefficient of Step 2: (a) real part, (b) imaginary part, (c) reflection coefficient.

By adding an open-ended rectangle ring on the back of Step 2, a stop band at 4.7 GHz and another band at 5.5 GHz are formed. As analyzed above, the length of the rectangle on the back is $L_5 + W_5/2$, which equals to half wavelength at 4.7 GHz. Treating it as an open-ended half wavelength transmission line, a parallel resonance circuit can be achieved. A series resonance circuit is added to match the impedance at 5.5 GHz. The equivalent circuit model is shown in Fig. 5. Z_{A2} represents the complex input impedance of Step 2. R_{eqi}, L_{eqi} and C_{eqi} are the resistor, inductor and capacitor values of the series and parallel resonant circuits respectively. The calculated and simulated input impedance and reflection coefficient of the equivalent circuit is depicted in Fig. 6. Good agreement is obtained.

Putting all the circuits together, as shows in Fig. 7, the results simulated by ADS and CST coincide with each other as described in Fig. 6. All the values of the circuit

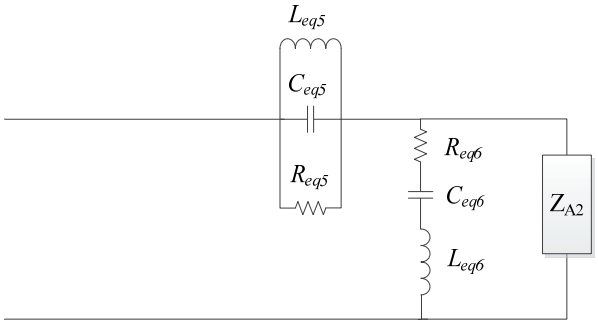

Fig. 5. Equivalent circuit model of Step 2 to Step 3. $R_{eq1} = 1376.9$ Ohm, $C_{eq1} = 5.9$ pF, $L_{eq1} = 0.19$ nH, $R_{eq2} = 73.26$ Ohm, $C_{eq2} = 0.216$ pF, $L_{eq2} = 5.32$ nH.

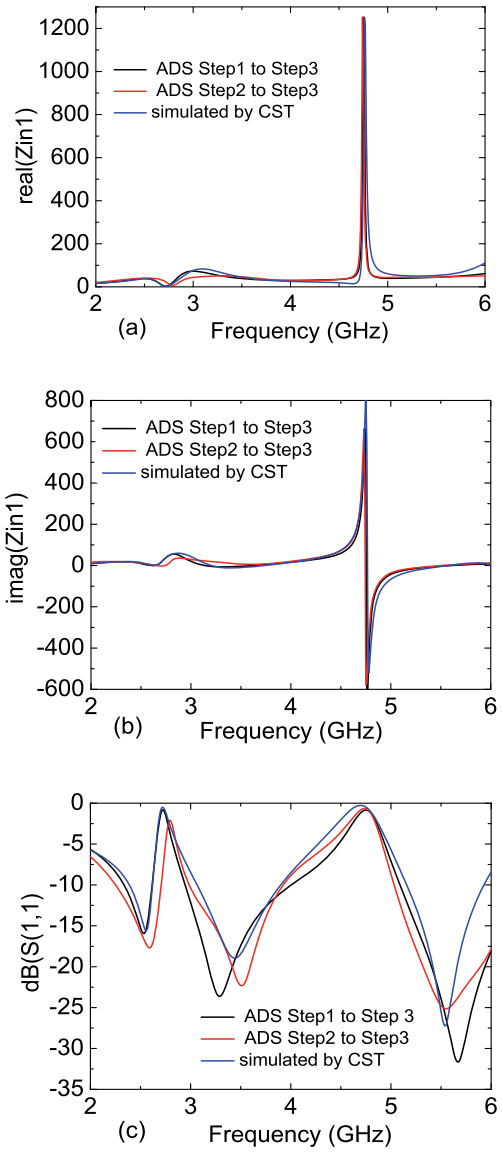

Fig. 6. Impedance and reflection coefficient of Step 3: (a) real part, (b) imaginary part, (c) reflection coefficient.

remain the same except $L_{eq1} = 0.38$ nH, $C_{eq3} = 3.71$ pF, $L_{eq4} = 4.96$ nH owing to the effect between rectangles on the back and front.

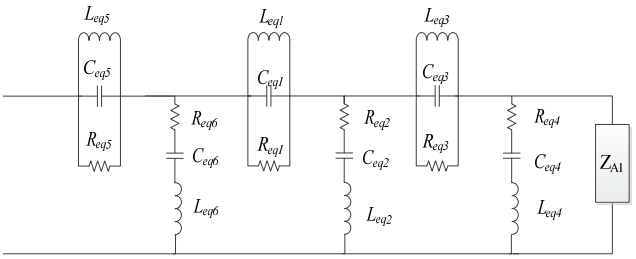

Fig. 7. Equivalent circuit model of Step 1 to Step 3.

Parameters	Value (mm)	Parameters	Value (mm)
L_{sub}	30	W_{sub}	26
L_1	19	W_1	3
L_2	14.5	W_2	1.5
L_g	7	W_3	21
L_5	13	W_4	12
L_f	10.4	W_5	14
g_5	0.3	W_6	1
W_f	3.8		

Tab. 1. Optimal dimensions of the designed antenna.

The optimal parameters are shown in Tab. 1. Fig. 8 shows the simulated and measured reflection coefficient. According to the results, it can be found that the proposed compact antenna effectively covers three separated impedance bandwidths of 220 MHz (2.33–2.55 GHz), 880 MHz (3.0–3.88 GHz) and 750 MHz (5.15–5.9 GHz), which can well satisfy both 2.4/5.2/5.5-GHz WLAN bands and 3.5/5.5-GHzWiMAX bands.

The simulated reflection coefficient is shown in Fig. 9(a) for different values of L_2. One can find that the band-notched frequency decreases with a little effect on the higher band around 3.7 GHz at the same time as L_2 increases, which elongates the slot and the inner square loop. Fig. 9(b) presents the simulated results of the proposed antenna with different L_5. The second notched- band shifts toward lower frequency when L_5 increased. As for the parameter W_5, it has the same effect as parameter L_5, which is shown in Fig. 9(c). Simulated and measured radiation patterns at 2.5, 3.5, and 5.5 GHz in the H-plane (xz-plane) and E-plane (yz-plane) of the proposed antenna are plotted in Fig. 10. These figures indicate the proposed antenna provides omni-directional radiation pattern in the xz-plane at the desired frequency bands. yz -plane radiation is bidirectional.

Fig. 11 illustrates the simulated current distributions on the antenna at 2.45, 2.7, 3.7, 4.7 and 5.5 GHz. Currents for the first band (i.e. 2.45 GHz) walk along the outside loop and the inner one mostly which means that the second rectangular loop enhance the current path comparing to Step1 and then the resonant frequency changes from 3 GHz to 2.45 GHz. At 2.7 GHz, it can be observed that the majority of the electric current flows on the both side of the slot equally and oppositely, which results in a notched band at this frequency. The electric current distributes on the inner square loop mostly at 3.7 GHz.

While at 4.7 GHz, the direction of the current on the back is contrary to that on the front patch. Then the notched band at 4.7 GHz is introduced. For 5.5 GHz it concentrates

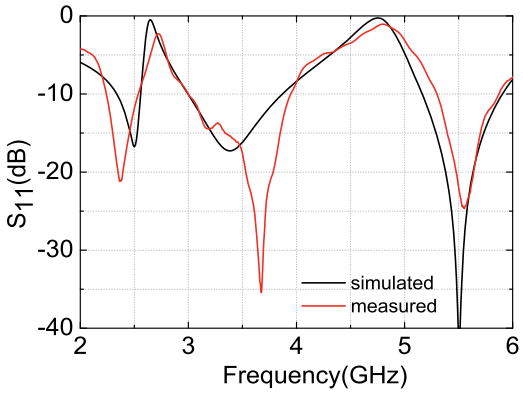

Fig. 8. Simulated and measured reflection coefficient of the antenna.

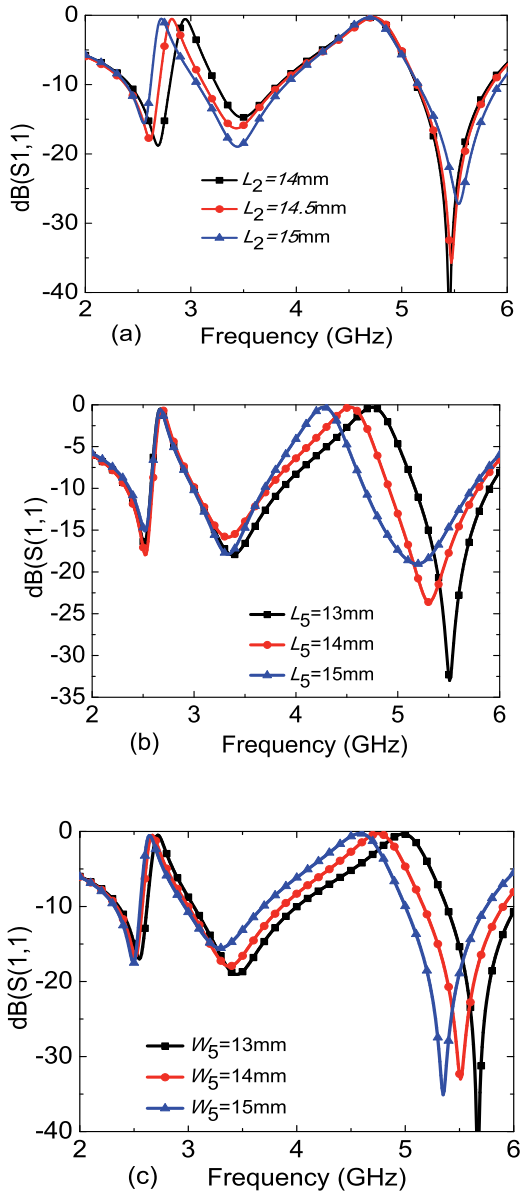

Fig. 9. Simulated reflection coefficient of the antenna with parameters: (a) L_2, (b) L_5, (c) W_5.

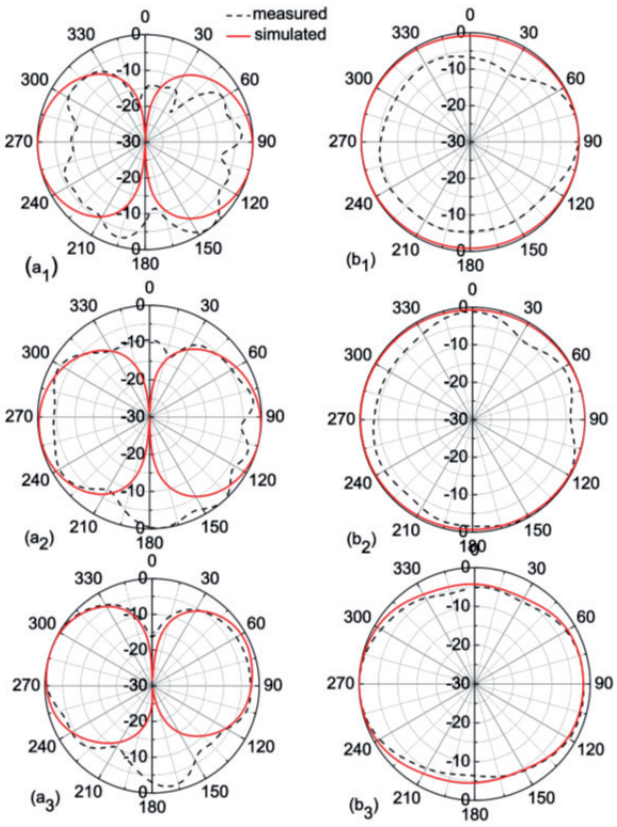

(a) E-plane (b) H-plane

Fig. 10. (a) Simulated and measured radiation patterns of the antenna for E-plane at (a_1) 2.5 GHz, (a_2) 3.5 GHz, (a_3) 5.5 GHz. (b) Simulated and measured radiation patterns of the antenna for H-plane at (b_1) 2.5 GHz, (b_2) 3.5 GHz, (b_3) 5.5 GHz.

around the square loop on the backside of the substrate mainly for coupling. Fig. 12 depicts the overall efficiency and the measured antenna gain versus frequency. The peak gain varies in a range of 1.08–1.39 dB of the lower band and 2.35–3.49 dB of the middle band and 2.46–3.28 dB of the upper band. The gain increases as frequency goes up, which is caused by the distortion of radio pattern. As a consequence, the omni-directional antenna develops into a quasi-directional one plotted in Fig. 10. The total efficiency of the three bands is 62% at 2.45 GHz, 70% at 3.5 GHz and 79% at 5.5 GHz respectively. The loss in connectors, the twisted cables and measurement tolerance may become bigger than the one in the lower band. So the efficiency varies slightly although antenna gain increases.

3 Conclusion

A triple-band monopole planar antenna with two square loops and a slit square loop for WLAN and WiMAX systems has been proposed and studied in this paper. Parameters sweep and the corresponding equivalent circuits' analysis are completed. There is a good agreement between simulated and measured results which indicate the multi-band planar antenna is suitable for applications as an internal antenna for portable devices which work during the frequency band of WLAN and WiMAX.

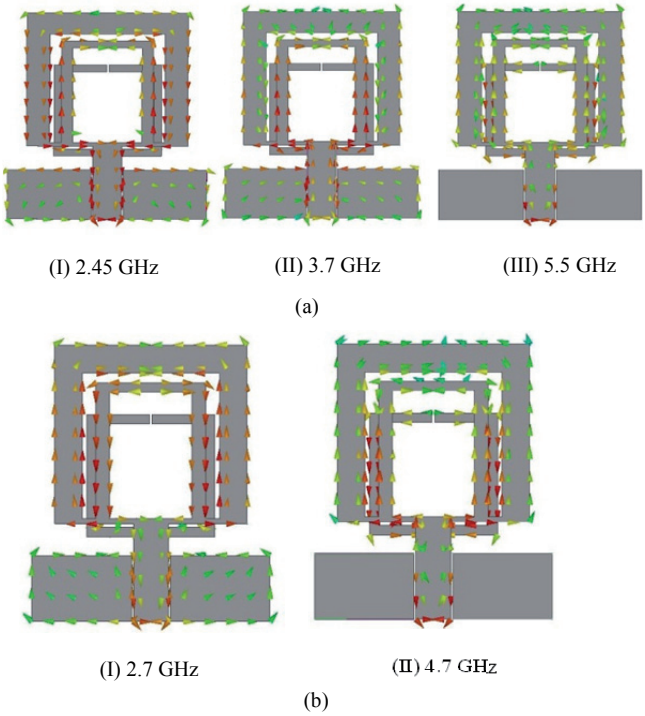

Fig. 11. (a) Surface current distribution for three pass bands: (I) 2.45 GHz, (II) 3.7 GHz, (III) 5.5 GHz. (b) Surface current distribution for two notched-bands: (I) 2.7 GHz and (II) 4.7 GHz.

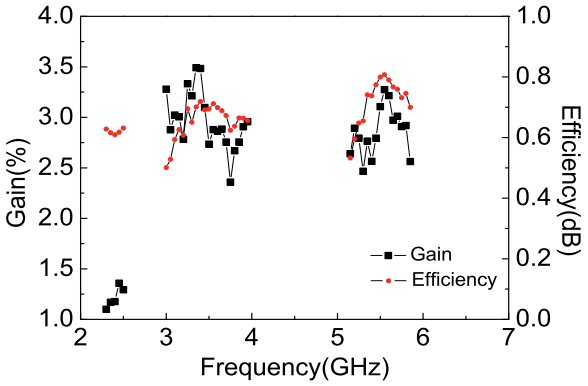

Fig. 12. Measured gain and efficiency of the antenna.

References

[1] CHIANG, M.J., WANG, S., HSU, C.C. Compact multi-frequency slot antenna design incorporating embedded arc-strip. *IEEE Antennas Wireless Propag. Lett.,* 2012, vol. 11, p. 834–837.

[2] CHANG, T.H., KIANG, J.F. Compact multi-band h-shaped slot antenna. *IEEE Trans. Antennas Propag.,* 2013, vol. 61, no. 8, p. 4345–4399.

[3] LIU, H.W., KU, C.H., YANG, C.F. Novel CPW-fed planar monopole antenna for WiMAX/WLAN applications. *IEEE Antennas Wireless Propag. Lett.,* 2010, vol. 9, p. 240–243.

[4] MOK, W.C., WONG, S.H., LUK, K.M., LEE, K.F. Single-layer single-patch dual-band and triple-band patch antennas. *IEEE Trans. Antennas Propag.,* 2013, vol. 61, no. 8, p. 4341–4344.

[5] BAE, H.R., SO, S.O., CHO, C.S., LEE, J.W., KIM, J. A crooked U-slot dual-band antenna with radial stub feeding. *IEEE Antennas Wireless Propag. Lett.,* 2009, vol. 8, p. 1345–1348.

[6] LIU, W.C., WU, C.M., TSENE, Y.J. Parasitically loaded CPW-fed monopole antenna for broadband operation. *IEEE Trans. Antennas Propag.,* 2011, vol. 59, no. 6, p. 2415–2419.

[7] ANTONIADES, M. A., ELEFTHERIADES, G. V. A compact multiband monopole antenna with a defected ground plane. *IEEE Antennas Wireless Propag. Lett.,* 2008, vol. 7, p. 652–655.

[8] ZHAI, H.Q., MA, Z.H., HAN, Y., LIANG, C.H. A compact printed antenna for triple-band WLAN/WiMAX applications. *IEEE Antennas Wireless Propag. Lett.,* 2013, vol. 12, p. 65–68.

[9] WONG, K.L., LEE, G.Y., CHIOU, T.W. A low-profile planar monopole antenna for multiband operation of mobile handsets. *IEEE Trans. Antennas Propag.,* 2003, vol. 51, no. 1, p. 121–125.

[10] BAEK, J.G., HWANG, K.C. Triple-band unidirectional circularly polarized hexagonal slot antenna with multiple L-shaped slits. *IEEE Trans. Antennas Propag.,* 2013, vol. 61, no. 9, p. 4831–4835.

[11] DENG, C.P., LIU, X.Y., ZHANG, Z. K., TENTZERIS, M. M. A miniascape-like triple-band monopole antenna for WLAN applications. *IEEE Antennas Wireless Propag. Lett.,* 2012, vol. 11, p. 1330–1333. DOI: 10.1109/LAWP.2012.2227292.

[12] FUGUO ZHU, GAO, S., HO, A.T.S., ABD-ALHAMEED, R.A., SEE, C.H., BROWN, T.W.C., JIANZHOU LI, GAO WEI, JIA-DONG XU. Multiple band-notched UWB antenna with band-rejected elements integrated in the feed line. *IEEE Trans. Antennas Propag.,* 2013, vol. 61, no. 8, p. 3952–3960. DOI: 10.1109/TAP.2013.2260119.

[13] SHARMA, V., SAXENA, V. K., SHARMA, K. B., BHATNAGAR, D. Multi-band elliptical patch antennas with narrow sector slot for WiMAX applications. *International Journal of Microwave and Optical Technology,* 2012, vol. 7, no. 2. p. 89–96.

[14] LOSITO, O., BOZZETTI, M., DIMICCOLI, V., BARLETTA, D. Multiple sector ring monopole antenna. In *Proceedings of the 6th European Conference on Antenna and Propagation.* Prague (Czech Rep.), 2012, p. 804–807.

About Authors …

Xiaolin YANG was born in Gansu, China, in 1974. He received the Ph.D. at Applied Physics from the Lanzhou University in 2005. He is currently an Associate Professor in School of Physical Electronics, University of Electronic Science and Technology of China (UESTC). His current research interests are microwave circuits and systems and ultra-wideband antenna.

Fangling KONG was born in Jiangxi Province, China. She received the Bachelor degree in Physics from GanNan Normal University, in 2012, and is currently working towards the M.S degree in Electronic and Communication Engineering at UESTC. Her research interests are in UWB antenna.

Xuelin LIU was born in Hunan Province, China. She received the Bachelor degree in Physics from HuNan Normal University, in 2012, and is currently working towards the M.S degree in Electronic and Communication Engineering at UESTC. Her research interests are in UWB antenna.

Chunyan SONG was born in Heibei Province, China. She received the Bachelor degree in Jiaotong from Southwest Jiaotong University, in 2009, and is currently working towards the M.S degree in Electronic and Communication Engineering at UESTC. Her research interests are in UWB antenna.